Hypoxia adipose stem cell-derived exosomes promote high-quality healing of diabetic wound involves activation of PI3K/Akt pathways

Jie Wang
Second Affiliated Hospital of Harbin Medical University
Hao Wu
Second Affiliated Hospital of Harbin Medical University
Yixuan Peng
Second Affiliated Hospital of Harbin Medical University
Yue Zhao
Second Affiliated Hospital of Harbin Medical University
Youyou Qin
Second Affiliated Hospital of Harbin Medical University
Yingbo Zhang
Second Affiliated Hospital of Harbin Medical University
zhibo xiao (zhiboxiaodoctor@126.com)
Second Affiliated Hospital of Harbin Medical University

Research Article

Keywords: Diabetic wound, Hypoxia, Exosomes, ADSCs, PI3K/AKT

Posted Date: May 26th, 2021

DOI: https://doi.org/10.21203/rs.3.rs-542843/v1

Version of Record: A version of this preprint was published at Journal of Nanobiotechnology on July 7th, 2021. See the published version at https://doi.org/10.1186/s12951-021-00942-0.

Abstract

Refractory diabetic wounds can cause persistent inflammation and delayed healing due to hypoxia. Currently, no optimal solution is available. Exosomes of adipose stem cells (ADSCs-exo) may promote skin wound healing, however, molecular mechanisms remains mysterious. We found significantly enhanced survival and proliferation of adipose stem cells after hypoxia induction compared to normoxia. Here, we aimed to investigate if hypoxic adipose stem cells exosomes (HypADSCs-exo) participate in hypoxia adaptability and accelerate diabetic wound healing. Based on high-throughput sequencing, 215 microRNAs (miRNAs) were upregulated and 369 miRNAs downregulated in HypADSCs-exo compared to ADSCs-exo. Up-regulated miR-21-3p, miR-126-5p, miR-31-5p whereas down-regulated gene miR-99b and miR-146-a correlated with wound healing. According to Gene Ontology (GO) and Kyoto Encyclopedia of Genes and Genomes (KEGG), these miRNAs might regulate cell metabolism, differentiation and Transforming growth factor-β (TGF-β) function. Consistently, HpyADSCs-exo could promote diabetic wounds healing and inhibit inflammation through PI3K/AKT signaling pathway. Collectively, HpyADSCs-exo may potentially be applied in clinical therapy as an alternative strategy to improve wound healing.

Introduction

For diabetes, molecular mechanisms underlying wound healing are complex and involve dysfunction of multiple signaling pathways and processes. In particular, diabetic wound is susceptible to infection and scarring, while non-union or slow healing becomes a major culprit that seriously affects patients' quality of life[1–4]. At initial stage of wound, cellular adaptability to hypoxia was decreased, resulting in persistent inflammation and substantially delayed healing[5]. At present, the treatment of diabetic wounds mainly focuses on advanced dressing, negative pressure, electrical stimulation, hyperbaric oxygen, and skin transplantation. However, therapeutic effect is not satisfactory, so it is necessary to identify an effective approach to expedite diabetic wound repair[6].

Adipose tissue-derived stem cells (ADSCs) are a group of pluripotent mesenchymal cells that can enhance wound healing through paracrine release of various cytokines and growth factors, thus affecting biological functions of skin fibroblasts. ADSCs hold a good prospect in wound repair[7]. Exosomes, extracellular vesicles with a diameter of 30 ~ 150 nm, mediate remote communication between cells. Exosomes can be transferred from a donor cell to recipient cells, delivering proteins, RNAs and DNAs[8,9]. Compared with cell therapy, exosomes may minimize immune mediated rejection and malignant transformation[10]. It is well established that hypoxia activates hypoxia-inducible factor (HIF-1α), which regulates transcription of angiogenic genes, such as vascular endothelial growth factor (VEGF) and VEGF receptors, to promote angiogenesis[11–13]. Interestingly, ADSCs-exo are involved in a wide range of biological processes by affecting tissue responses to injury, infection and diseases[14–19]. ADSCs secrete more exosomes under hypoxic environment, while HypADSCs-exo can improve blood perfusion and survival of transplanted tissues and reduce inflammatory filtration in adipose[20–23]. A variety of miRNA in exosomes especially play an important role in promoting wound healing of diabetes[24,25].

Although evidence on high-quality skin wound healing is still lacking at this stage, these results provide a new perspective for HypADSCs-exo in soft tissue repair.

In this study, we performed high-throughput sequencing on ADSCs-exo and HypADSCs-exo to identify differentially expressed miRNAs. Notably, HypADSCs-exo induced proliferation, collagen metabolism and migration through PI3K/AKT signaling pathway in human skin fibroblasts. Furthermore, we established a diabetic wound model in nude mice to analyze speed and quality of wound tissue healing, and to explore molecular mechanism underlying beneficial effects of HypADSCs-exo. Collectively, our study provides a new theoretical basis for wound healing and a promising strategy for cell-free therapy.

Results

Characterization of ADSCs-exo

Under transmission electron microscopy, ADSCs-exo were round vesiculas (Fig. 1A), expressing specific markers HSP70 and CD9 (Fig. 1B), with an average size of 110 nm (Fig. 1C). Exosomes labeled with PKH26 red fluorescent dyes were localized around the nucleus, indicating that ADSCs-exo were internalized by fibroblasts (Fig. 1D).

3.2 Expression Profiles of miRNAs in ADSCs-exo and HypADSCs-exo

Differential expression profiles of miRNAs were described in Fig. 2. As shown in Fig. 2A and 2B, clustered heat map and volcano plot of differentially expressed miRNAs depicted up- and down-regulated miRNAs in HypADSCs-exo, compared to ADSCs-exo. 369 miRNAs were downregulated whereas 215 upregulated as presented by Volcano Plot filtering. Downstream genes of differentially expressed miRNAs were analyzed with GO and KEGG. GO enrichment was shown in Fig. 3A and 3B. The most common biological process was regulation of macromolecule metabolism (GO:0060255). The most enriched cellular component was perinuclear region of cytoplasm (GO:0048471). The most enriched molecular function was binding (GO:0005488). As shown in Fig. 3C, KEGG pathway analysis revealed thyroid hormone signaling pathway as the most enrichment factor.

HypADSCs-exo promotes fibroblast proliferation and migration in vitro

Based on scratch assay, migration of fibroblast was increased gradually for 24 h after treatment with different concentrations of exosomes (Fig. 4A). Similar result was demonstrated by transwell assay (Fig. 4B). HypADSCs-exo significantly promoted fibroblast proliferation (Fig. 4C)

HypADSCs-exo regulate fibroblast chemokines and extracellular matrix formation

Expression of HypADSCs-exo proteins in fibroblasts was significantly increased (Fig. 5A). ADSC-exo gene expression of COLI, TGF-β, EGF and bFGF was significantly increased in fibroblasts (Fig. 5B). As a result, HypADSCs-exo regulated the production of extracellular proteins and chemokines in fibroblasts and exerted potential effects on angiogenesis.

Regulation of PI3K/AKT signaling in fibroblast

PI3K/AKT signaling pathway promotes cell proliferation, migration and wound healing. To investigate if PI3K/AKT could regulate behaviors of fibroblasts, we pretreated fibroblasts with Ly294002 (PI3K/AKT inhibitor). Accordingly, AKT phosphorylation induced by HypADSCs-exo was significantly inhibited (Fig. 5C). Upon inhibiting PI3K/AKT signaling, HypADSCs-exo mediated proliferation of fibroblast was significantly attenuated (Fig. 5D). Thus, proliferation and migration of fibroblasts regulated by HypADSCs-exo might be dependent on PI3K/AKT signaling.

HypADSCs-exo accelerate skin wound healing in diabetic mice

We established a diabetic wound model with nude mice. From the images taken on days 0, 3, 7 and 14, respectively, the wound size of DW-hexo group was significantly smaller than that of DW-hexo, DW or Ctrl (Fig. 6A). In DW-hexo group, wounds were almost completely closed on day 14. As for wound closure rate, HypADSCs-exo treated wounds contracted much faster than ADSCs-exo treated wounds on days 7 and 14. Additionally, HypADSCs-exo treated skin wounds had complete re-epithelialization and cuticle covering on the epidermis as demonstrated by blue skin fibers (Fig. 6B). By contrast, skin wounds treated with ADSCs-exo exhibited less re-epithelialization.

HypADSCs-exo regulate inflammatory factors, chemokines and extracellular matrix formation in diabetic mice

In wound tissue of DW-hexo group, upregulated expression of collagens and growth factors (TGF-β, PDGF, COLI and VEGF) in skin tissue cells could accelerated wound healing (Fig. 7A). Potential effects of DW-hexo on stromal-related factors CD31, TGF-β, COLI, COL□ as well as inflammatory factor IL-6 in diabetic wound were investigated. Interestingly, expression of CD31, TGF-β, COLI and COL□ was upregulated while IL-6 was downregulated in DW-hexo treatment group at week 2 (Fig. 7B), in comparison with DW-exo, DW or Ctrl.

Discussion

Incidence and prevalence of diabetes keep rising globally[26]. Because of slow healing and even non-healing, diabetic wound has brought a great challenge to therapy[27]. Diabetic patients with foot ulcers are 2.5 times more likely to die in five years[28]. Therefore, it is necessary to explore molecular mechanisms underlying diabetic wound healing and to identify effective treatment of diabetic wound. Importantly, ADSCs together with conditioned medium may promote skin wound healing and regeneration[29,30]. Compared with adipose stem cell transplantation, ADSCs-exo has greater potential, and ADSCs-exo under hypoxia has advantages in promoting angiogenesis and bone healing compared with that under normorxia[31,32]. In this study, we have demonstrated that HypADSCs-exo promotes fibroblast proliferation and migration by activating PI3K/AKT pathway, which can accelerate healing of diabetic wounds.

In the early stage of diabetic healing, cells adapt to hypoxia; while in the late stage, inflammatory response and growth factors directly affect the process of wound healing[33–35]. Therefore, we analyzed differential expression of miRNAs and related pathways, cell functions and target proteins between hypoxic exosomes and normoxic exosomes with high-throughput sequencing. 215 miRNAs were upregulated whereas 369 downregulated in hypoxic exosomes compared with normoxic exosomes. Upregulated miR-21-3p/miR-126-5p/miR-31-5p whereas down-regulated miR-99b/miR-146-a might play a role in promoting fibroblast proliferation and migration, as well as in regulating immune response by activating targeted signaling pathways[36,37]. GO and KEGG indicate regulatory effects of adipose stem cell exosomes on cell metabolism, differentiation and TGF-β secretion under hypoxia, partially through activating PI3K/AKT and MARK pathways. Thus, we propose HypADSCs-exo can accelerate diabetic wound healing. Consistently, HypADSCs-exo can regulate inflammation and extracellular matrix secretion, partially through PI3K/AKT signal pathway, to accelerate wound healing in diabetes. This finding provides a new solution for refractory diabetic wounds.

Fibroblasts are the main target and effector cells in skin wounds[3]. Skin fibroblasts interact with keratinocytes, adipocytes, mast cells and extracellular matrix (including collagen)[38,39]. Accordingly, HypADSCs-exo induced proliferation and migration of fibroblasts. HypADSCs-exo also increases production of extracellular matrix and growth factors. PI3K/AKT signaling pathway is involved in regulating cell proliferation and migration, while exosomes can activate PI3K/AKT for survival[40,41]. Notably, HypADSCs-exo induce AKT fast channels, which can be weakened by Ly294002, suggesting that survival-promoting signals in fibroblasts can weaken HypADSCs-exo fast channels to improve cell viability. ADSCs-hexo induced fibroblast proliferation and migration partially depends on PI3K/AKT pathway. Besides, TGF-β stimulates fibroblast proliferation in coordination with bFGF[42]. EGF as a chemokine promotes fibroblast proliferation and migration[43]. In our study, TGF-β, EGF, COLI, bFGF induced by HypADSCs-exo were increased significantly in fibroblasts. HypADSCs-exo may regulate the expression of multiple growth factors, to promote the proliferation and migration of fibroblasts, as well as angiogenesis.

A diabetic wound model using nude mouse was developed and treated with HypADSCs-exo *in vivo*. It's noteworthy that HypADSCs-exo can accelerate high-quality healing of diabetic wounds compared with

ADSCs-exo. It's well-known that extracellular matrix plays a supporting and elastic role in wound healing and regeneration, depending on the secretion of collagen I and III. HypADSCs-exo may regulate extracellular matrix formation, thereby accelerating wound healing in diabetes. The expression of IL-6 was decreased in wound tissue of HypADSCs-exo treated diabetic nude mice, while the expression of VEGF was increased. These results suggest that HypADSCs-exo may play a key role in extracellular matrix remodeling during wound healing and thus partially improving scar fibrosis. We detected a significant increase in TGF-β, COLI, PDGF and VEGF expression in HypADSCs-exo treated diabetic mice. In this regard, VEGF has the potential to initiate angiogenesis and promote wound healing[44]. PDGF released by platelets binds to fibroblast surface receptors during wound repair[45]. HypADSCs-exo may promote skin regeneration by regulating the secretion and expression of growth factors. Meanwhile, the expression of CD31 was up-regulated, indicating increased angiogenesis. Taken together, HypADSCs-exo may accelerate high-quality healing of diabetic wound, which provides the possibility for clinical application of HypADSCs-exo .

Nevertheless, our study has some limitations. For example, potential effects of specific miRNAs derived from HypADSCs-exo on fibroblasts need further investigation. Moreover, PI3K/AKT signaling may not be the only pathway in HypADSCs-exo that affects fibroblasts, which requires illustration. Furthermore, clinical application of HypADSCs-exo requires more accurate injection dose and time to achieve an optimal therapeutic efficacy.

Conclusion

Collectively, HypADSCs-exo may accelerate the rate of diabetic wound healing, improve the quality of wound healing whereas inhibit inflammation. HypADSCs-exo may induce proliferation and migration of fibroblasts, partially by activating PI3K/AKT signaling pathway, and thus enhancing the secretion of vascular growth factors and extracellular matrix. These results provide a new treatment strategy by applying HypADSCs-exo in diabetic wound repair.

Materials And Methods

Sample collection and cell culture

Subcutaneous adipose and skin tissue samples were harvested from the abdomen of women (aged 20 to 50 years) who received liposuction from January to May 2020 at the Second Affiliated Hospital of Harbin Medical University. Informed consent was obtained from each subject. This study was approved by Institutional Review Board (IRB) of the Second Affiliated Hospital of Harbin Medical University and conducted according to the *Declaration of Helsinki* principles. Acquisition of human subcutaneous fat aimed to establish primary culture of adipose stem cells. The cell pellet was resuspended in Dulbecco's Modified Eagle Medium F12 (DMEM/F12; Corning, New York, USA) supplemented with 10% fetal bovine serum (FBS; Gibco, Thermo Fisher Scientific, Rockville, MD, USA) and 100 IU penicillin/100 mg/mL streptomycin (Solarbio, Beijing, China), and cultured in a humidified 5% CO_2 atmosphere at 37°C. Primary

cultures of human fibroblasts (HFs) from surgical specimens were established. Cells from passages 3 to 8 were used for experiments. Cells were maintained in DMEM supplemented with 10% FBS and 5 mM l-glutamine, 100 U/ml penicillin, and 100 mg/mL of streptomycin in a 5% CO2 incubator at 37°C.

Isolation and analysis of exosomes

Human ADSCs (hADSCs) at 70%-80% confluence were washed with PBS and cultured in microvascular endothelial cell growth medium-2 media deprived of FBS with supplement of 1 × serum replacement solution (PeproTech) for 24 hours. Then, supernatant was centrifuged 300×g for 10 min and 2000×g for 10 min to remove dead cells and debris. 5 ml of ExoQuick-TC reagent (System Biosciences) was mixed with 10 mL of supernatant. After centrifugation at 1500×g for 30 minutes, the exosome-containing pellet was resuspended in nuclease-free water. TRIzol-LS (Invitrogen, California, USA) and Exosomal Protein Extraction kit (Invitrogen, USA) were used to extract total RNA and protein, respectively. Exosomes were either applied immediately for experiments or stored at −80°C. Dimensions of purified exosomes were determined with NanoSight LM10 (Malvern Instruments) nanoparticle tracking system. Levels of HSP70 and CD9 proteins were detected by Western blotting (abcam, USA). ADSCs-exos were labeled using PKH26 Red Fluorescent Cell Linker Kits according to the manufacturer's instructions (Sigma, USA). Specific concentrations of proteins in exosomes were assessed with bicinchoninic acid assay kits (Beyotime, China). Ultrastructure of extracellular vesicles was analyzed by Transmission electron microscopy (TEM) with Libra 120 instrument (Zeiss).

MiRNA high-throughput sequence

Exosomes' miRNAs were isolated with Total exosomes RNA Separation Kit (Qiagen's exoRNeasy Serum Plasma Kit) and analyzed by sequencing. RNA integrity was verified on a Bioanalyzer 2100 using Agilent RNA 6000 Nano Assay. Accurate quantification for sequencing was determined with qPCR-based KAPA Biosystems Library Quantification kit (Kapa Biosystems, Inc., Woburn, Mass.). Each library was diluted to a final concentration of 10nM and pooled equimolar before clustering. Paired-end sequencing was performed on all samples. Quality analysis of genes included coverage graph and thermal graph. All samples met inclusion criteria.

Enrichment Analysis

GO (http://www.geneontology.org) and KEGG (http:// www.genome.jp/kegg) databases were used to predict possible functions of differentially expressed mRNAs and to explore potential pathways. GO and KEGG analyses for differentially expressed miRNAs identified downstream genes regulated by miRNAs. A *P* value of <0.05 and |log2 (fold-change)| >1 were defined as statistically significant. The calculation of a *P* value for GO analysis was performed using the following equation:

$$P = 1 - \sum_{i-0}^{m-1} \frac{\binom{M}{i}\binom{N-M}{n-i}}{\binom{N}{n}}$$

RNA extraction and real-time PCR

Total RNA was isolated from hADSCs using RNAiso Plus (TaKaRa Biotechnology, Shiga, Japan) according to the manufacturer's instructions. Isolated RNA was subsequently transcribed to cDNA using First Strand cDNA Synthesis Kit (Thermo Scientific). Next, mRNA expression was measured via real-time PCR with ABI Prism 7500 Sequence Detection System (ABI, CA, USA) using SYBR Premix ExTaq (TaKaRa Biotechnology). QPCR was performed as follows: initial incubation at 95°C for 2 min, followed by 40 cycles of 95°C for 5 s and 55°C for 30 s. A melt curve was analyzed to determine specificity of the reaction. Each sample was tested in triplicate. Relative expression level was measured with $2^{-\Delta\Delta Ct}$ method. Primer sequences were listed (Supporting Information Table 1).

Human fibroblasts (HF)treatment

To investigate proliferation and migration of HFs treated with ADSCs-exo, HypADSCs-exo (100 μg/mL) or PBS (control) were incubated with 5×10^6 HFs. To explore molecular mechanisms, cells were pretreated with a PI3K/AKT inhibitor, Ly294002 (50nM, MedChemExpress, Monmouth Junction, NJ, USA), for 1h before treatment with ADSCs-exo, HypADSCs-exo or PBS. Cells were harvested 30min after treatment for Western blotting or after 48h for Edu assay, respectively.

Cell proliferation assay

The Edu colorimetric immunoassay kit (Cell Proliferation ELISA, Roche Diagnostics, Germany) was used for quantification of cell proliferation according to manufacturer's instructions. Cell proliferation was expressed as the mean percentage of the control values (set at 100%)

Western blot analysis

Total separated proteins from control, ADSCs-exo, HypADSCs-exo or PBS (100 μg/mL) induced HFs for 48 hours were lysed using cell lysis buffer [20mM Tris (pH 7.5), 150mM sodium chloride, 1% Triton X-100, 2.5mM sodium pyrophosphate, 1mM ethylenediaminetetraacetic acid, 1% sodium carbonate, 0.5 μg/ml leupeptin, and 1mM phenylmethanesulfonyl fluoride (PMSF)]. The lysate was collected with a scraper and centrifuged at 12,000 rpm at 4°C for 15 min. Total protein samples (20μg) were loaded onto 12% or 15% sodium dodecyl sulfate polyacrylamide gel for electrophoresis, and transferred onto polyvinyl difluoride transfer membranes (Roche, USA) at 0.8 mA/cm^2 for 60 min. Membranes were blocked at 37°C for 1h with blocking solution. Then, samples were incubated overnight at 4°C with primary antibodies against β-actin (ab8226, Abcam), Type I collagen (COL I) (ab34710, Abcam), Type □ collagen (COL □) (ab184993, Abcam), P-AKT (13038, Cell Signaling Technology) and AKT (9272, Cell Signaling

Technology), in blocking solution at a compatible dilution. Membranes were washed for three times (10 min each time) in Tris-buffered saline Tween-20 and incubated for 2h at room temperature with anti-rabbit and anti-mouse secondary antibodies (Abcam) in blocking solution at a dilution of 1:8000. After being washed for three times (10min each time) in Tris-buffered saline Tween-20, bands were detected using Enhanced Chemiluminescence kit (Beyotime BioTech, Shanghai, China) according to the manufacturer's protocol. Images were visualized with ImageQuant LAS 4000 mini machine (GE).

Cell migration

Human fibroblasts (HFs) were seeded in 12-well plates (2×10^5 cells/well) and incubated at 37 ℃ until 90% confluence. The confluent monolayer was scratched using a 200μl pipette tip and washed with PBS to remove the debris and smooth the edge of the scratch. Then, serum-free EBM-2 medium (500μl) with exosomes (50μg/ml ADSCs-exo, HypADSCs-exo) or PBS was added to each well. Cells were photographed (t = 0h, 12h and 24h, respectively). Cell migration was measured by the ratio of closure area to initial wound area (t = 0h) as follows: migration area (%) = $(A_0 - A_n)/A_0 \times 100$, where A_0 represented the area of initial wound, while A_n represented the residual area of wound at the metering point (t = nh).

Transwell experiment was performed according to the manufacturer's recommendations. Simply, a total of 1×10^4 HFs per group were seeded on the upper chamber of the transwell (Corning Inc., NY, USA) with 100 μL of serum-free medium. 500μL of medium containing 10% serum exosomes-free, ADSCs-exo, HypADSCs-exo or PBS were added to the lower layer. After incubation for 24h, HFs on the permeable membrane of the upper chamber were fixed with anhydrous ethanol, stained by crystal violet, washed three times and wiped to remove non-migrated cells. Then, migrated cells on the underside of the membrane were counted manually under a light microscope.

Diabetic wound healing evaluation

All experiments were carried out with the approval of IACUC at the Second Hospital of Harbin Medical University. BALB/c mice (4 weeks old, weight:16 ± 2 g) were obtained from the Second Affiliated Hospital of Harbin Medical University and fed with 45% high fat diet for 5 weeks. After fasting for 12h without food and water, the mice were intraperitoneally injected with streptozotocin (35mg/kg in 0.1M citrate-buffered saline, pH 4.5) to induce Diabetes Mellitus (DM). Glucose was measured with blood sugar test paper (Roche, Basel, Switzerland). Glucose level >16.7 mmol/L indicated DM. To establish a stable animal model of DM, diabetic nude mice were re-fed with high-fat diet for 4 week and blood glucose levels were reconfirmed before wound formation. Anesthesia was performed with intraperitoneal injection of 10% chloral hydrate solution (250μL/100g). A square full thick skin injury (0.8 cm ×0.8 cm) was produced on the back of each nude mice. Then diabetic nude mice were randomly divided into 3 groups, respectively, in which ADSCs-exo (DW+exo), HypADSCs-exo (DW+hexo) (2mg in 100μL PBS) or 100μL PBS (DW) were subcutaneously injected into four mid-points of the wound edge. Normal nude mice (Ctrl) with normal diet and water received the same wound operation. The wound was photographed on days 0,

3, 7 and 14, respectively after surgery to observe the healing process. Image J software was used to analyze wound size on days 0, 3, 7 and 14, respectively. Wound closure rate was calculated by formula: wound closure (%) = $(A_0-A_t)/A_0\times100\%$, where A0 was the wound size at day 0 while A_t was the wound size at indicated day.

Histology

The harvested tissue specimens were immediately fixed in 4% paraformaldehyde solution for paraffin embedding. Then, 4-μm-thick tissue sections were incubated with primary antibodies against β-actin, CD31, COL□, IL-6, or TGF-β overnight at 4 °C and with secondary antibodies (Abcam) for 1 h at 37 °C. The sections were stained with 3,3-diaminobenzidine and counter stained with hematoxylin. Immunofluorescence staining on COLI (1:100; ab34710) was performed. Hematoxylin-eosin (H&E) and Masson's trichrome staining were conducted. The expression levels of COLI, TGF-β, PDGF and VEGF mRNA in tissues of nude mice were detected by qRT-PCR. All primer sequences were listed in table 1. Images were obtained using a Leica microscope. We randomly selected five locations with different visual fields for each image.

Statistical analysis

All data were expressed as mean ± standard deviation (SD). Non-parametric one-way ANOVA was used for comparison between three or more groups. Statistical significance was considered when a p value was <0.05. GraphPad Prism 6.0 software and Image J were used for all statistical analyses.

Abbreviations

Adipose stem cells exosomes (ADSCs-exo); Hypoxic adipose stem cells exosomes (HypADSCs-exo); Basic fibroblast growth factor (bFGF); Collegen □ (COL I); Collegen □ (COL III); Control (Ctrl); Diabetic wound (DW); Diabetic wound exosomes (DW+exo); Diabetic wound hypoxic exosomes (DW+hexo); Dulbecco's Modified Eagle Medium F12 (DMEM/F12); Fetal bovine serum (FBS); Gene Ontology (GO); Hypoxia inducible factor-1α (HIF-1α); Human fibroblast (HF); Hematoxylin and eosin (H&E); Institutional Review Board (IRB); Interleukin-6 (IL-6); Kyoto Encyclopedia of Genes and Genomes (KEGG); Stromal cell-derived factor-1(SDF-1); Transforming growth factor-β (TGF-β); Transmission electron microscopy (TEM); Phosphate-AKT (P-AKT); Phenylmethanesulfonyl fluoride (PMSF); Platelet derived growth factor (PDGF); Quantitative reverse transcription-polymerase chain reaction (qRT-PCR); Standard deviation (SD); Vascular endothelial growth factor (VEGF)

Declarations

Competing interests

The authors declare that they have no competing interests

Acknowledgments

The authors thank the scientifific research center at the Second Affifiliated Hospital of Harbin Medical University for technical support. They also extend a special thanks to the Experimental Animal Center of the Second Affifiliated Hospital of Harbin Medical University for helping with our animal experiments.

Funding

This work was supported by the National Natural Science of China (Grant 81471796) and Heilongjiang Province Science Foundation for Excellent Youth Scholars (Grant JC2017019).

Availability of data and materials

The data that support the findings of this study are available from the corresponding author upon reasonable request.

Author contributions

Z.X., J.W. and H.W. designed and performed experiments. J.W. and H.W. contributed to data compilation and paper preparation. Z.X., J.W., H.W., Y.P., Y.Q., Y.Z. provided critical feedback on the study and contributed to the preparation of the paper. Z.X. and J.W. devised the study and oversaw the research program. All authors listed reviewed the paper and provided feedback.

Ethics approval

This study was approved by the Institutional Review Board of the Second Hospital of Harbin Medical University and conducted in accordance with the 2000 Helsinki Declaration. All experiments involving animals were approved by the Animal Ethics Committee of the Second Hospital of Harbin Medical University.

References

1. Francia P, Anichini R, Seghieri G, De Bellis A, Gulisano M. History, Prevalence and Assessment of Limited Joint Mobility, from Stiff Hand Syndrome to Diabetic Foot Ulcer Prevention: A Narrative Review of the Literature. *Curr Diabetes Rev*. 2018;14(5):411-426.
2. Hamed S, Ullmann Y, Masoud M, Hellou E, Khamaysi Z, Teot L. Topical erythropoietin promotes wound repair in diabetic rats. *J Invest Dermatol*. 2010;130(1):287-294.
3. Singer AJ, Clark RA. Cutaneous wound healing. *N Engl J Med*. 1999;341(10):738-746.
4. Lan CC, Wu CS, Huang SM, et al. High-glucose environment reduces human β-defensin-2 expression in human keratinocytes: implications for poor diabetic wound healing. *Br J Dermatol*. 2012;166(6):1221-1229.

5. Pankajakshan, D., Agrawal, D.K., 2014. Mesenchymal stem cell paracrine factors in vascular repair and regeneration. J. Biomed. Technol. Res. 1.
6. Boateng J, Catanzano O. Advanced Therapeutic Dressings for Effective Wound Healing–A Review. *J Pharm Sci*. 2015;104(11):3653-3680.
7. Hu ZC, et al. Randomized clinical trial of autologous skin cell suspension combined with skin grafting for chronic wounds. *Br J Surg*. 2015;102(2):e117-e123
8. Park BS, Jang KA, Sung JH, et al. Adipose-derived stem cells and their secretory factors as a promising therapy for skin aging. *Dermatol Surg*. 2008;34(10):1323-1326.
9. Vu NB, Nguyen HT, Palumbo R, Pellicano R, Fagoonee S, Pham PV. Stem cell-derived exosomes for wound healing: current status and promising directions [published online ahead of print, 2020 Dec 2]. *Minerva Med*. 2020;10.23736/S0026-4806.20.07205-5.
10. Colombo M, Raposo G, Théry C. Biogenesis, secretion, and intercellular interactions of exosomes and other extracellular vesicles. *Annu Rev Cell Dev Biol*. 2014;30:255-289.
11. Majmundar AJ, Wong WJ, Simon MC. Hypoxia-inducible factors and the response to hypoxic stress. *Mol Cell*. 2010;40(2):294-309.
12. Ding J, Wang X, Chen B, Zhang J, Xu J. Exosomes Derived from Human Bone Marrow Mesenchymal Stem Cells Stimulated by Deferoxamine Accelerate Cutaneous Wound Healing by Promoting Angiogenesis. *Biomed Res Int*. 2019;2019:9742765.
13. An Y, Lin S, Tan X, et al. Exosomes from adipose-derived stem cells and application to skin wound healing. *Cell Prolif*. 2021;54(3):e12993.
14. Yu M, Liu W, Li J, et al. Exosomes derived from atorvastatin-pretreated MSC accelerate diabetic wound repair by enhancing angiogenesis via AKT/eNOS pathway. *Stem Cell Res Ther*. 2020;11(1):350.
15. Lee Y, El Andaloussi S, Wood MJ. Exosomes and microvesicles: extracellular vesicles for genetic information transfer and gene therapy. *Hum Mol Genet*. 2012;21(R1):R125-R134.
16. Wu J, Wang Y, Li L. Functional significance of exosomes applied in sepsis: A novel approach to therapy. *Biochim Biophys Acta Mol Basis Dis*. 2017;1863(1):292-297.
17. Szatanek R, Baj-Krzyworzeka M, Zimoch J, Lekka M, Siedlar M, Baran J. The Methods of Choice for Extracellular Vesicles (EVs) Characterization. *Int J Mol Sci*. 2017;18(6):1153.
18. Phinney DG, Pittenger MF. Concise Review: MSC-Derived Exosomes for Cell-Free Therapy [published correction appears in Stem Cells. 2017 Sep;35(9):2103]. *Stem Cells*. 2017;35(4):851-858.
19. Vlassov AV, Magdaleno S, Setterquist R, Conrad R. Exosomes: current knowledge of their composition, biological functions, and diagnostic and therapeutic potentials. *Biochim Biophys Acta*. 2012;1820(7):940-948.
20. Han YD, Bai Y, Yan XL, et al. Co-transplantation of exosomes derived from hypoxia-preconditioned adipose mesenchymal stem cells promotes neovascularization and graft survival in fat grafting. *Biochem Biophys Res Commun*. 2018;497(1):305-312.

21. Xue C, Shen Y, Li X, et al. Exosomes Derived from Hypoxia-Treated Human Adipose Mesenchymal Stem Cells Enhance Angiogenesis Through the PKA Signaling Pathway. *Stem Cells Dev*. 2018;27(7):456-465.
22. Liu W, Yu M, Xie D, et al. Melatonin-stimulated MSC-derived exosomes improve diabetic wound healing through regulating macrophage M1 and M2 polarization by targeting the PTEN/AKT pathway. *Stem Cell Res Ther*. 2020;11(1):259.
23. Geiger A, Walker A, Nissen E. Human fibrocyte-derived exosomes accelerate wound healing in genetically diabetic mice. *Biochem Biophys Res Commun*. 2015;467(2):303-309.
24. Huang J, Yu M, Yin W, et al. Development of a novel RNAi therapy: Engineered miR-31 exosomes promoted the healing of diabetic wounds. *Bioact Mater*. 2021;6(9):2841-2853.
25. Lv Q, Deng J, Chen Y, Wang Y, Liu B, Liu J. Engineered Human Adipose Stem-Cell-Derived Exosomes Loaded with miR-21-5p to Promote Diabetic Cutaneous Wound Healing. *Mol Pharm*. 2020;17(5):1723-1733.
26. Chatterjee S, Khunti K, Davies MJ. Type 2 diabetes [published correction appears in Lancet. 2017 Jun 3;389(10085):2192]. *Lancet*. 2017;389(10085):2239-2251.
27. Boulton AJ, Vileikyte L, Ragnarson-Tennvall G, Apelqvist J. The global burden of diabetic foot disease. *Lancet*. 2005;366(9498):1719-1724.
28. Walsh JW, Hoffstad OJ, Sullivan MO, Margolis DJ. Association of diabetic foot ulcer and death in a population-based cohort from the United Kingdom. *Diabet Med*. 2016;33(11):1493-1498.
29. Hocking AM, Gibran NS. Mesenchymal stem cells: paracrine signaling and differentiation during cutaneous wound repair. *Exp Cell Res*. 2010;316(14):2213-2219.
30. Yang JA, Chung HM, Won CH, Sung JH. Potential application of adipose-derived stem cells and their secretory factors to skin: discussion from both clinical and industrial viewpoints. *Expert Opin Biol Ther*. 2010;10(4):495-503.
31. Han Y, Ren J, Bai Y, Pei X, Han Y. Exosomes from hypoxia-treated human adipose-derived mesenchymal stem cells enhance angiogenesis through VEGF/VEGF-R [published correction appears in Int J Biochem Cell Biol. 2020 Sep;126:105805]. *Int J Biochem Cell Biol*. 2019;109:59-68.
32. Zhang Y, Hao Z, Wang P, et al. Exosomes from human umbilical cord mesenchymal stem cells enhance fracture healing through HIF-1α-mediated promotion of angiogenesis in a rat model of stabilized fracture. *Cell Prolif*. 2019;52(2):e12570.
33. Noor S, Zubair M, Ahmad J. Diabetic foot ulcer--A review on pathophysiology, classification and microbial etiology. *Diabetes Metab Syndr*. 2015;9(3):192-199.
34. Braun L, Kim PJ, Margolis D, Peters EJ, Lavery LA; Wound Healing Society. What's new in the literature: an update of new research since the original WHS diabetic foot ulcer guidelines in 2006. *Wound Repair Regen*. 2014;22(5):594-604.
35. Markuson M, Hanson D, Anderson J, et al. The relationship between hemoglobin A(1c) values and healing time for lower extremity ulcers in individuals with diabetes. *Adv Skin Wound Care*. 2009;22(8):365-372.

36. Casado-Díaz A, Quesada-Gómez JM, Dorado G. Extracellular Vesicles Derived From Mesenchymal Stem Cells (MSC) in Regenerative Medicine: Applications in Skin Wound Healing. *Front Bioeng Biotechnol*. 2020;8:146. Published 2020 Mar 3.
37. Zhang D, Xuan J, Zheng BB, et al. Metformin Improves Functional Recovery After Spinal Cord Injury via Autophagy Flux Stimulation. *Mol Neurobiol*. 2017;54(5):3327-3341.
38. Kim WS, Park BS, Sung JH, et al. Wound healing effect of adipose-derived stem cells: a critical role of secretory factors on human dermal fibroblasts. *J Dermatol Sci*. 2007;48(1):15-24.
39. Olczyk P, Mencner Ł, Komosinska-Vassev K. The role of the extracellular matrix components in cutaneous wound healing. *Biomed Res Int*. 2014;2014:747584.
40. Vrijsen KR, Maring JA, Chamuleau SA, et al. Exosomes from Cardiomyocyte Progenitor Cells and Mesenchymal Stem Cells Stimulate Angiogenesis Via EMMPRIN. *Adv Healthc Mater*. 2016;5(19):2555-2565.
41. Kim S, Lee SK, Kim H, Kim TM. Exosomes Secreted from Induced Pluripotent Stem Cell-Derived Mesenchymal Stem Cells Accelerate Skin Cell Proliferation. *Int J Mol Sci*. 2018;19(10):3119.
42. Piazuelo E, Lanas A, Jimenez P, García-Gonzalez A, Esteva F. In vitro wound repair by human gastric fibroblasts: implications for ulcer healing. *Dig Dis Sci*. 1998;43(6):1230-1240.
43. Clark RA, McCoy GA, Folkvord JM, McPherson JM. TGF-beta 1 stimulates cultured human fibroblasts to proliferate and produce tissue-like fibroplasia: a fibronectin matrix-dependent event. *J Cell Physiol*. 1997;170(1):69-80.
44. Narayanan R, Huang CC, Ravindran S. Hijacking the Cellular Mail: Exosome Mediated Differentiation of Mesenchymal Stem Cells. *Stem Cells Int*. 2016;2016:3808674.
45. Werner S, Grose R. Regulation of wound healing by growth factors and cytokines. *Physiol Rev*. 2003;83(3):835-870.

Tables

Table. 1 Primer sequences of the study

hADSCs Genes	Forward primer 5′→3’	Reverse primer 5′→3’
Actin-Mouse	CACTGTCGAGTCGCGTCC	TCATCCATGGCGAACTGGTG
Actin-Human	TGGCACCCAGCACAATGAA	CTAAGTCATAGTCCGCCTAGAA
bFGF-Human	AAGAGCGACCCTCACATCAA	ACGGTTAGCACACACTCCTT
COLI-Human	GAGGGCAACAGCAGGTTCACTTA	TCAGCACCACCGATGTCCA
TGF-β-Human	GTGAGCTAGATCGGTTGCTT	CTTGCTAGATGGGAACTGAGAC
VEGF-Human	GGCGAAGAGAAGAGACACATT	TTCAATGGTGTGAGGACATAGG
TGF-β-Mouse	CGAAGCGGACTACTATGCTAAA	TCCCGAATGTCTGACGTATTG
VEGF-Mouse	AGGCTGCTGTAACGATGAAG	TCTCCTATGTGCTGGCTTTG
COLI-Mouse	GCACGCCCAGTTTGGTAT	TCACACAAGTCCCTATCCATTA
PDGF-Mouse	TAACACCAGCAGCGTCAAGT	TTCCCTACGCCTTCCTGTCT

Figures

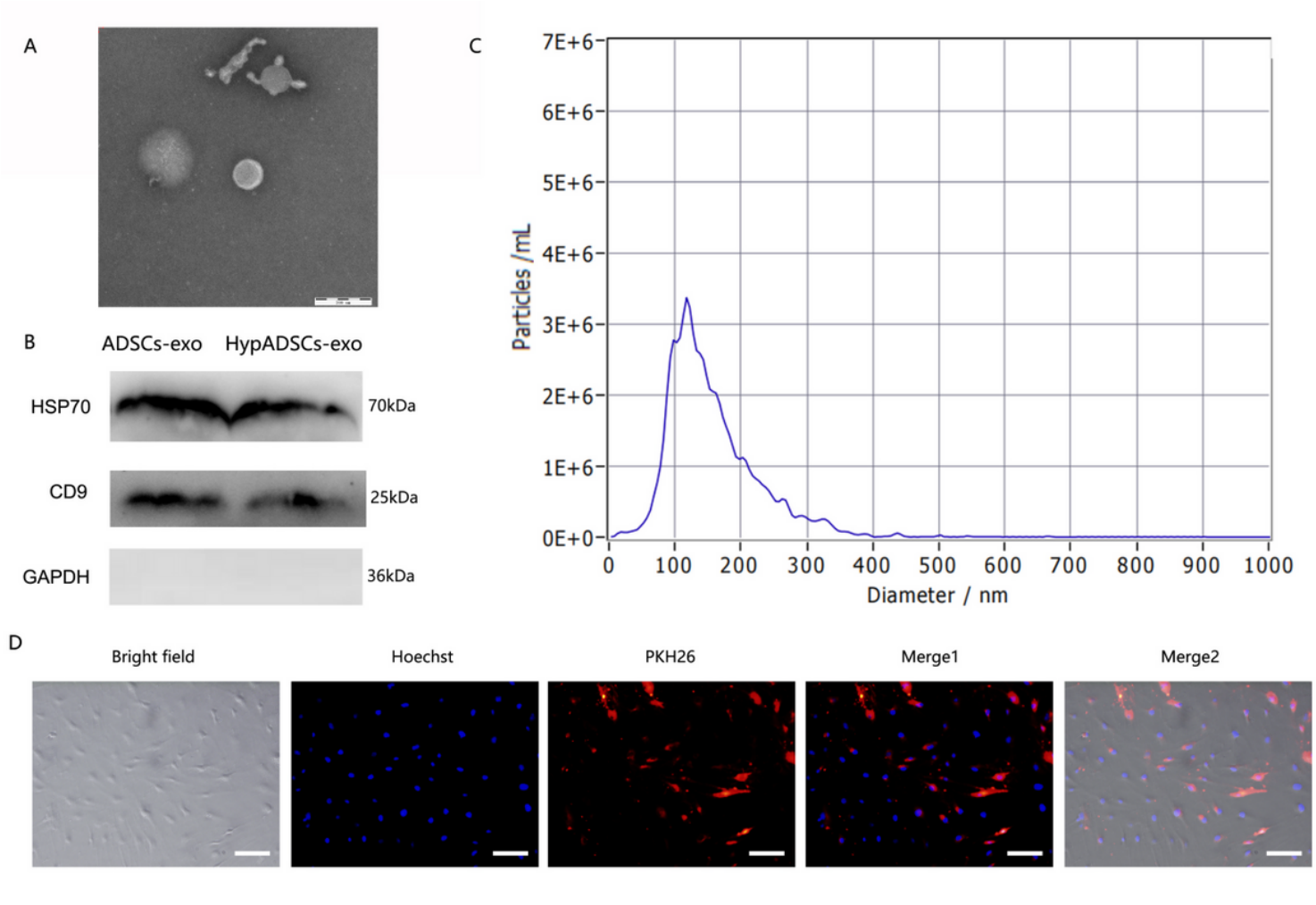

Figure 1

Characterization of ADSCs-exo. (A) Morphology observed under transmission electron microscope. (B) Particle size distribution. (C) Western blot was used to detect exosomes surface markers. (D) Fluorescent microscopy analysis of PKH26-labeled ADSCs-exo internalization by tenocytes. Bars, 100μm.

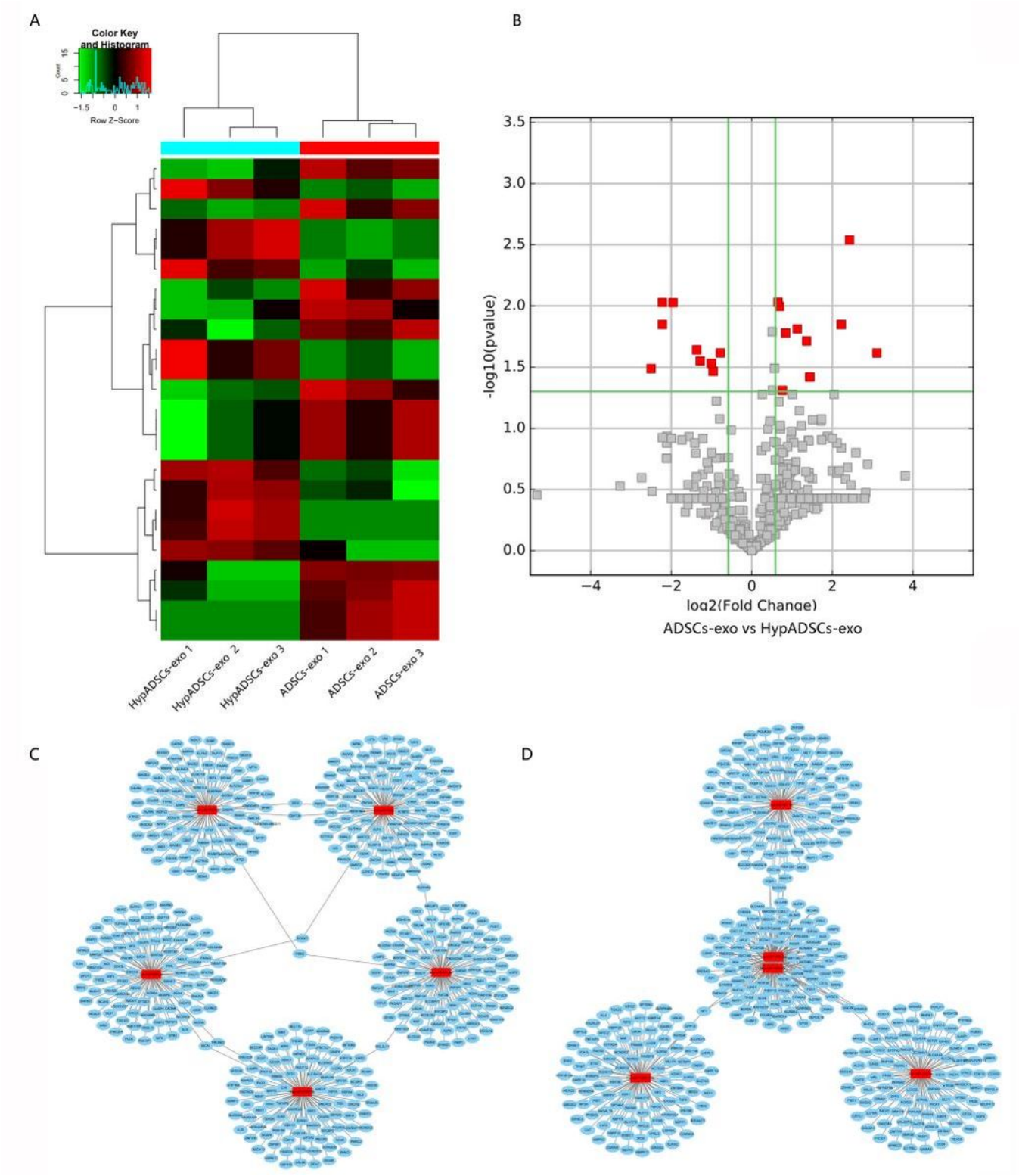

Figure 2

High-throughput sequencing analysis ADSCs-exo and HypADSCs-exo miRNA differential expression. (A) Clustered heat map of differentially expressed miRNAs depicting up and down regulated miRNAs . (B) Volcano plot of differentially expressed miRNAs depicting up and down regulated miRNAs. (C, D) Schematic representation of the predicted target genes and corresponding cellular functions of the miRNAs (C: up-regulated miRNAs and D: down-regulated miRNA) senriched in exosomes.

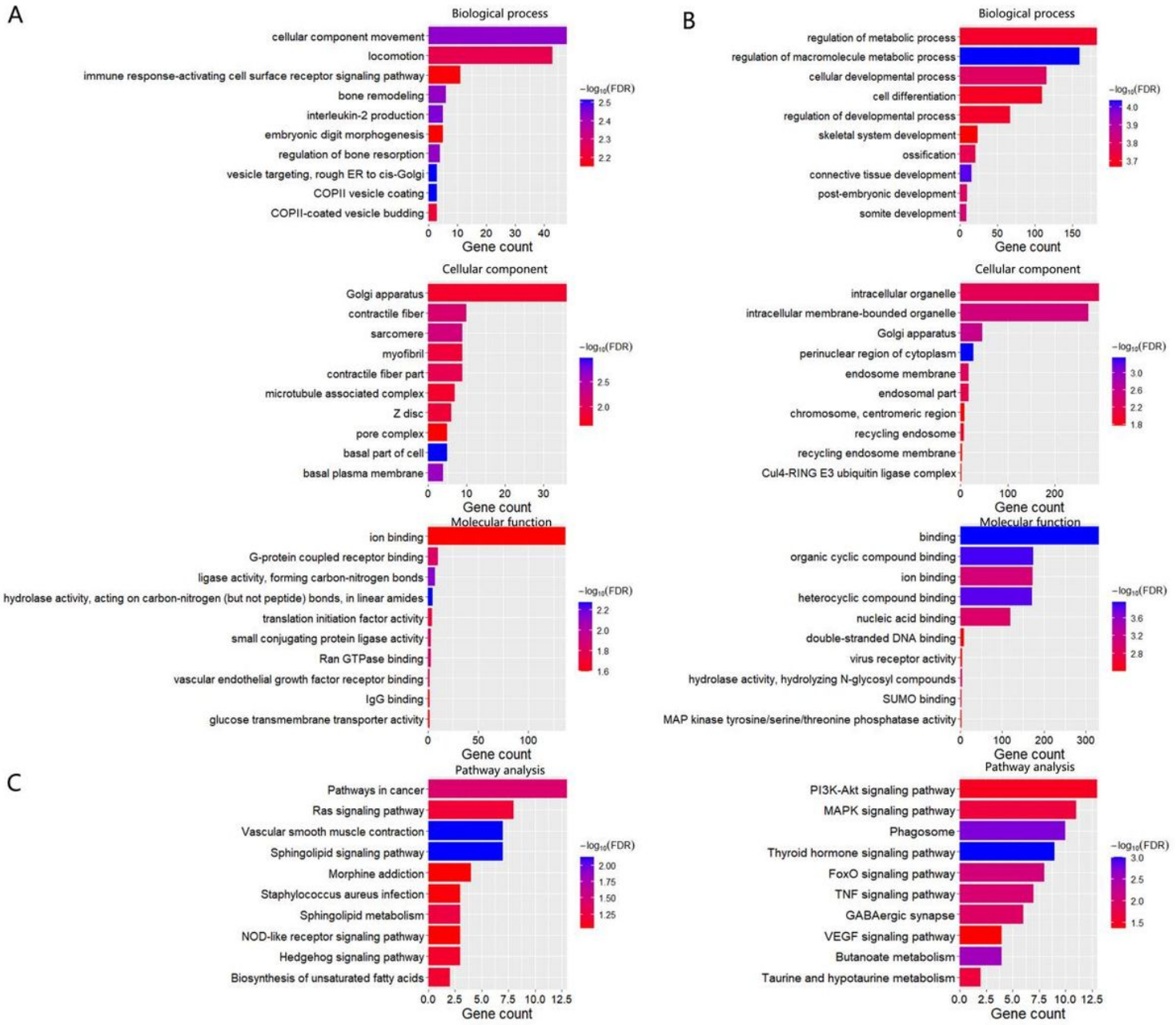

Figure 3

GO and KEGG enrichment of differentially expressed miRNAs. (A) GO enrichment of down-regulation expressed miRNAs. (B) GO enrichment of up-regulation expressed miRNAs. (C) Significant terms in KEGG pathways, the left is down-regulation, the right is up-regulation. n=3.

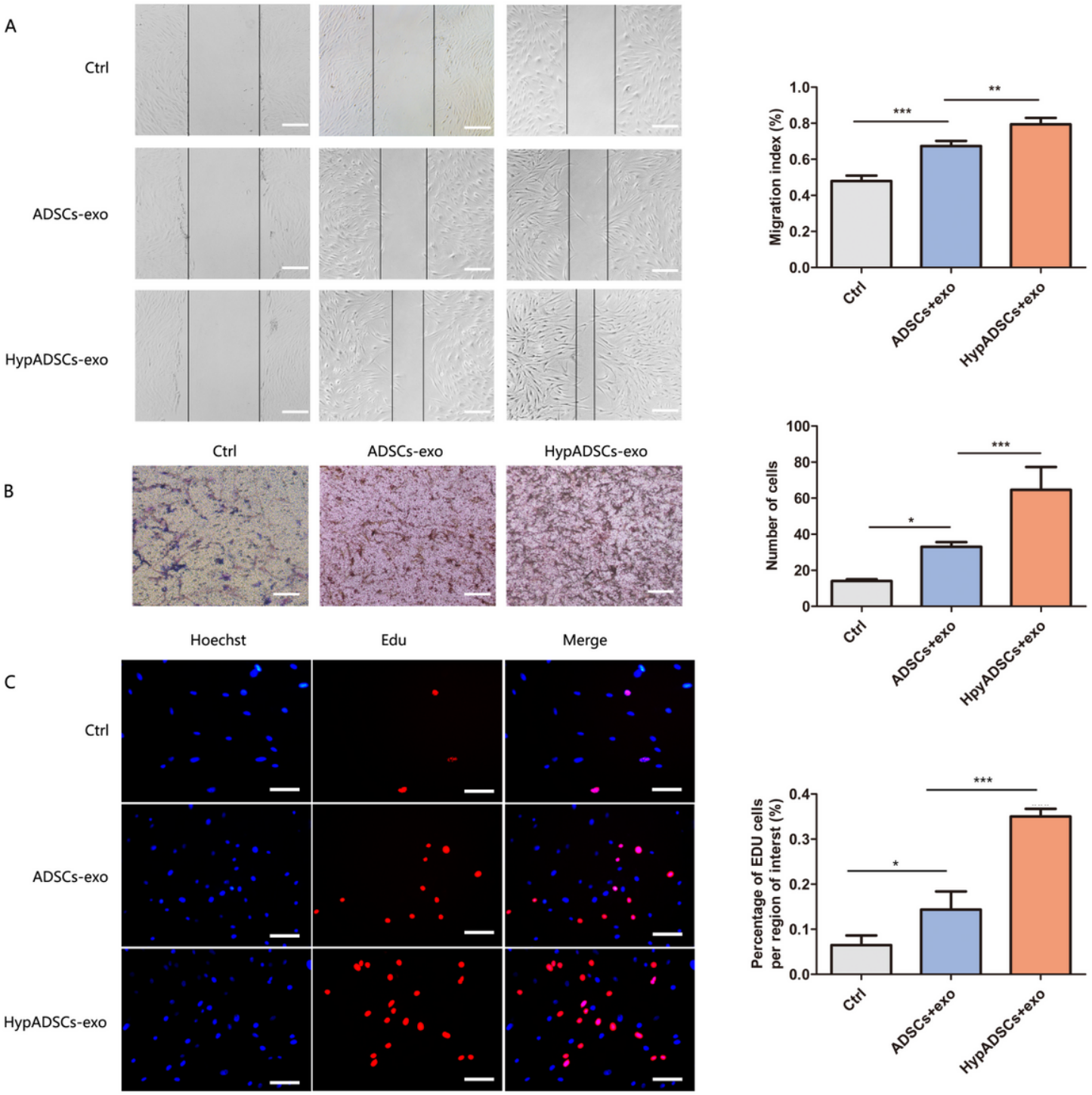

Figure 4

HypADSCs-exo significantly promote the proliferation and migration of HF. (A, B) The migration ability of HF treated with HypADSCs-exo, measured by scratch and Transwell test assays. (C) The proliferation of cells by Edu assays. Bars, 25 μm. Data are represented as mean ± SD. n = 3. *P < 0.01, **P < 0.001, ***P < 0.0001. Scale bars, 100μm.

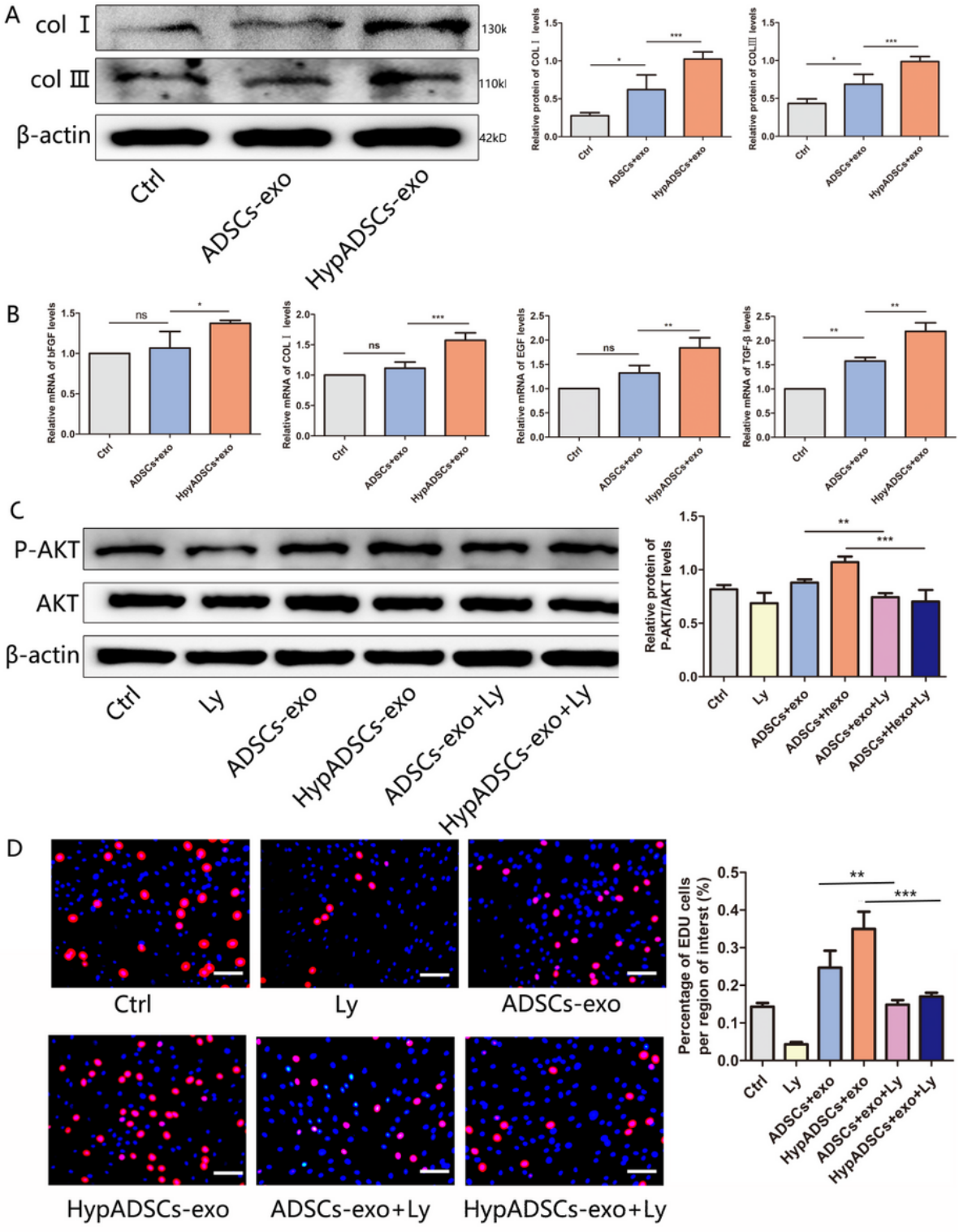

Figure 5

HypADSCs-exo promote the expression and secretion of extracellular matrix and growth factors in HF. (A) Analysis of protein expression levels in treated HF. (B) QRT-PCR analysis of mRNA levels, including bFGF, PDGF, COL□, EGF. Data are represented as mean ± SD. *, vs ADSCs-exo ; #, vs Ctrl. (C) Western-blot analysis of protein levels of P-AKT induced by different concentrations of control, ADSCs-exo and HypADSCs-exo. Ly294002 inhibit the activation of PI3K/ AKT induced by control, ADSCs-exo and

HypADSCs-exo, respectively. (D) Edu assay showed that HypADSCs-exo-mediated HF proliferation was suppressed by inhibitors Ly294002, compared with ADSCs-exo. Data are represented as mean ± SD. *P < 0.01, **P < 0.001, ***P < 0.0001. Scale bars, 100μm.

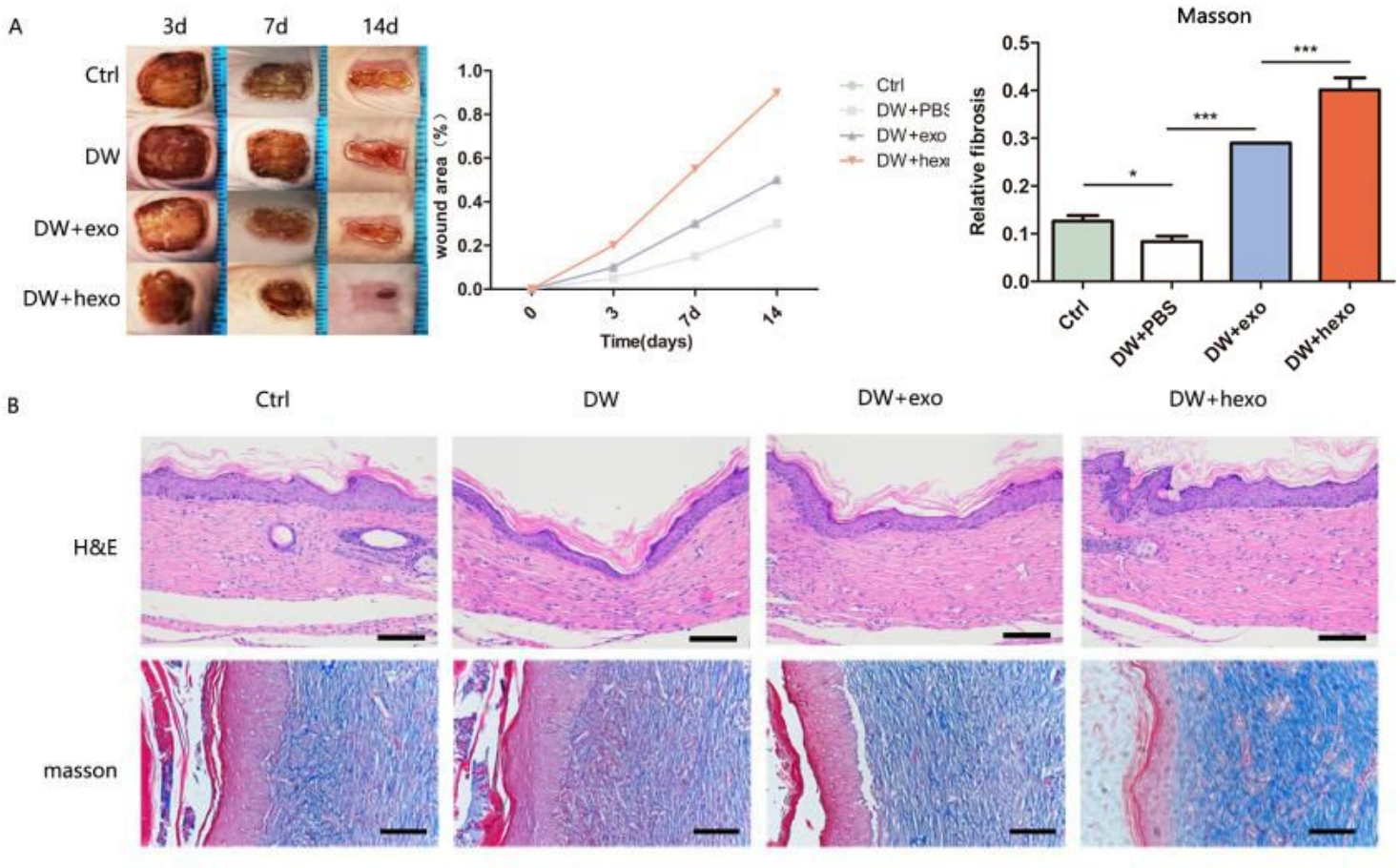

Figure 6

Observation of wound healing quality and velocity after operation. (A) After HypADSCs-exo treatment 0, 3, 7 and 14 days were taken. (B) HE staining of tissue wounds 14 days after operation. Masson staining of tissue wounds 14 days after operation. Data are represented as mean ± SD. *P < 0.01, **P < 0.001, ***P < 0.0001. Scale bars, 100μm.

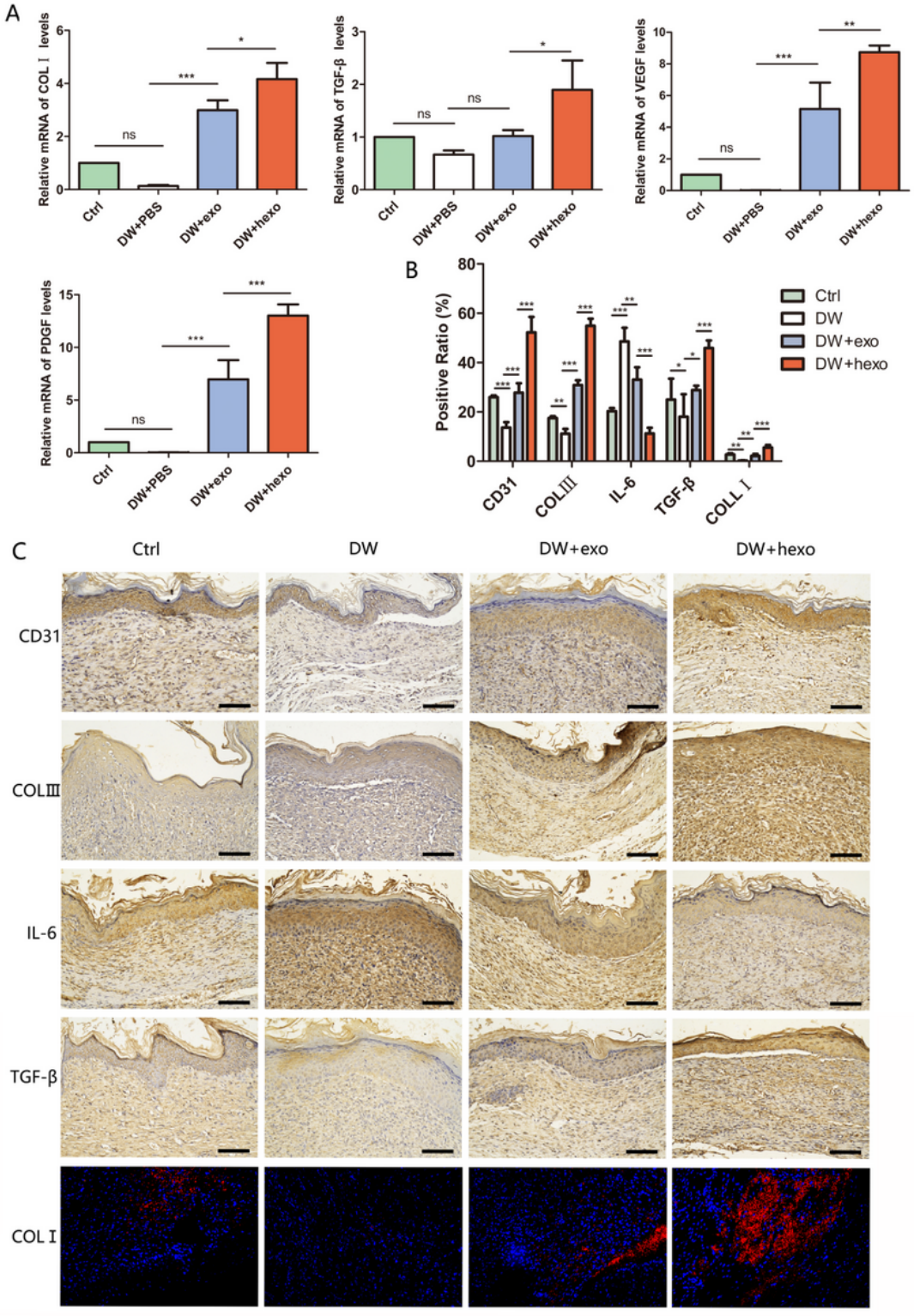

Figure 7

Genetic and histological analysis of wound healing in diabetes (A) QRT-PCR analysis of wound tissue mRNA level 14 days after operation, including COL□, TGF-β, VEGF, PDGF. (B, C) Expression of CD31, COL□, IL-6, TGF-β, COL□ in wound tissue was observed 21 days after operation. Data are represented as mean ± SD. *P < 0.01, **P < 0.001, ***P < 0.0001. Scale bars, 100μm.

Supplementary Files

This is a list of supplementary files associated with this preprint. Click to download.

- graphicalabstract.tif